



Synthesis, Characterization, Antioxidant, and Antibacterial Activities of 2-Aminochalcones and Crystal Structure of (2E)-1-(2-aminophenyl)-3-(4-ethoxyphenyl)-2-propen-1-one

Pumsak Ruanwas, Suchada Chantrapromma & Hoong-Kun Fun

To cite this article: Pumsak Ruanwas, Suchada Chantrapromma & Hoong-Kun Fun (2015) Synthesis, Characterization, Antioxidant, and Antibacterial Activities of 2-Aminochalcones and Crystal Structure of (2E)-1-(2-aminophenyl)-3-(4-ethoxyphenyl)-2-propen-1-one, Molecular Crystals and Liquid Crystals, 609:1, 126-139, DOI: [10.1080/15421406.2014.950003](https://doi.org/10.1080/15421406.2014.950003)

To link to this article: <http://dx.doi.org/10.1080/15421406.2014.950003>



Published online: 11 Apr 2015.



Submit your article to this journal [↗](#)



Article views: 51



View related articles [↗](#)



View Crossmark data [↗](#)

Synthesis, Characterization, Antioxidant, and Antibacterial Activities of 2-Aminochalcones and Crystal Structure of (2*E*)-1-(2-aminophenyl)-3-(4-ethoxyphenyl)-2-propen-1-one

PUMSAK RUANWAS,¹ SUCHADA CHANTRAPROMMA,^{1,*}
AND HOONG-KUN FUN^{2,3}

¹Department of Chemistry and Center of Excellence for Innovation in Chemistry, Faculty of Science, Prince of Songkla University, Hat-Yai, Songkhla, Thailand

²X-ray Crystallography Unit, School of Physics, Universiti Sains Malaysia, Penang, Malaysia

³Department of Pharmaceutical Chemistry, College of Pharmacy, King Saud University, Riyadh, Saudi Arabia

Five 2-aminochalcone derivatives [R = H(1), R = OCH₂CH₃(2), R = 2,4,5-OCH₃(3), R = 3,4,5-OCH₃(4), and R = thiophene(5)] were synthesized and characterized by ¹H NMR, FT-IR, and UV-Vis spectroscopy. Crystal structure of 2 was also determined by single crystal X-ray diffraction. Compound 2 crystallizes in a monoclinic P2₁/n space group with the unit cell parameters a = 32.804(7) Å, b = 4.9972(11) Å, c = 21.7173(3) Å, β = 128.440(4)°, V = 2788.4(10) Å³, and Z = 8. There are two molecules in an asymmetric unit of 2, the molecular structure of 2 is twisted with the dihedral angle between the two phenyl rings being 13.6(3)° in one molecule and 7.1(3)° in the other. In the crystal packing, the molecules of 2 are linked into chains along the b-axis by C–H...O interactions. Antioxidant and antibacterial activities of 1–5 were also carried out.

Keywords Antioxidant; antibacterial; chalcones; crystal structure; heteroaryl

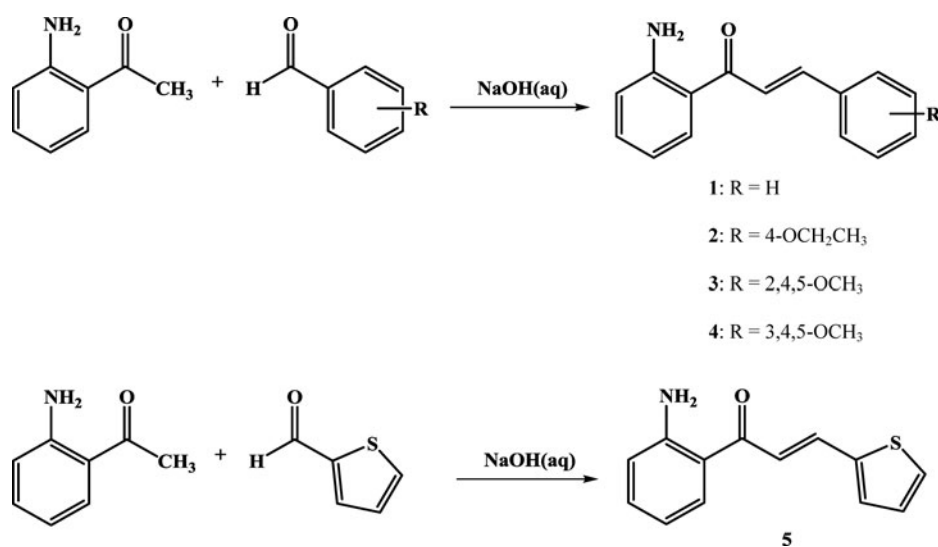
Introduction

Reactive oxygen species and free radicals, including the superoxide radical (O₂^{•−}), hydroxyl radical (OH), hydrogen peroxide (H₂O₂), and lipid peroxide radicals, are generated in the human body and they are considered to be implicated in a number of disease processes, including inflammatory, metabolic disorders, cellular aging, reperfusion damage, and cancer [1–3]. Antioxidants are the agents, which can inhibit or delay the oxidation of an oxidisable substrate in a chain reaction. Antioxidants are the first line of defense against free radical damage and are critical for maintaining optimum health. The basic structure

*Address correspondence to Suchada Chantrapromma, Department of Chemistry and Center of Excellence for Innovation in Chemistry, Faculty of Science, Prince of Songkla University, Hat-Yai, Songkhla 90112, Thailand. E-mail: suchada.c@psu.ac.th

Color versions of one or more of the figures in the article can be found online at www.tandfonline.com/gmcl.

of chalcones consists of two aromatic ring bridge by an α,β -unsaturated carbonyl group, a unique template associated with various applications such as antibacterial [4], antifungal [5], anti-inflammatory [6], anti-HIV-1 protease inhibition [7] antitumor [8], and electroactive fluorescent properties [9–10]. Moreover due to the presence of the reactive keto vinylenic group, chalcones, and their analogs have been reported to be antioxidants [11]. In this work, five derivatives of 2-aminochalcones (**1–5**) (Scheme 1) with different substitutions on the B-ring (Fig. 1) were synthesized and screened for antibacterial and antioxidant activities by the 2,2-diphenyl-1-picrylhydrazyl radical (DPPH) scavenging method [12]. In addition, the crystal structure of **2** was also carried out by single crystal X-ray diffraction. Compounds **1–5** exhibited antioxidant activity whereas our biological testing found that **1–5** are inactive against the tested bacteria strains which are *Bacillus subtilis*, *Enterococcus faecalis*, *Staphylococcus aureus*, methicillin-resistant *Staphylococcus aureus*, vancomycin-resistant *Enterococcus faecalis*, *Pseudomonas aeruginosa*, *Salmonella typhi*, and *Shigella sonnei*. Herein, we report the synthesis, characterization, antioxidant, and antibacterial activities of **1–5** and the crystal structure of **2**.



Scheme 1. Synthesis of compounds **1–5**.

Materials and Methods

All the chemical reagents and solvents were of analytical grade, purchased commercially, and used without further purification. Melting point was recorded in °C and measured using an electrothermal melting point apparatus. Infrared spectra were recorded by using FTS 165 FT-IR spectrophotometer. Ultraviolet–Visible (UV–Vis) absorption spectra were recorded using a Shimadzu UV-2450 UV-Visible spectrophotometer. The ¹H NMR spectra were recorded on 300 MHz Bruker FTNMR Ultra Shield spectrometer in CDCl₃ with TMS as the internal standard. Chemical shifts reported in ppm are expressed in hertz. Antioxidant was carried out by using Anthos 2010 Microplate Absorbance Reader.

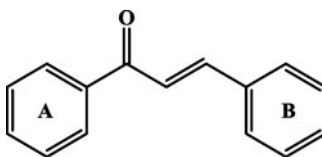


Figure 1. Basic structure of chalcones.

Synthesis of the Compounds

Compounds **1–5** were synthesized by mixing 2-aminoacetophenone (3 mmol) and the corresponding benzaldehyde (3 mmol) in ethanol (30 mL) [benzaldehyde for (**1**); 4-ethoxybenzaldehyde for (**2**); 2,4,5-trimethoxybenzaldehyde for (**3**); 3,4,5-trimethoxybenzaldehyde for (**4**); and 2-thiophenecarboxaldehyde for (**5**)], 30% NaOH aqueous solution (5 mL) was then added and the mixture was stirred at room temperature for 2 hr. The obtained precipitate was filtered and washed with distilled water.

(2E)-1-(2-aminophenyl)-3-phenyl-2-propen-1-one (**1**). Orange powder (92% yield), mp 128–129°C, UV-Vis (CHCl₃) λ_{max} (nm): 234.46, 318.57, FT-IR (KBr) ν (cm⁻¹): 3428 (N–H stretching), 2536 (C–H aromatic stretching), 1607 (C=O stretching), 1576 (C=C aromatic stretching), ¹H NMR 300 Hz, (CDCl₃) δ (ppm): 7.64 (*d*, *J* = 7.8 Hz, 2H, aromatic ring), 7.32 (*t*, *J* = 7.8 Hz, 2H, aromatic ring), 7.06 (*t*, *J* = 7.8 Hz, 1H, aromatic ring), 8.16 (*d*, *J* = 15.2 Hz, 1H, *trans*-H), 7.56 (*d*, *J* = 15.2 Hz, 1H, *trans*-H), 5.62 (*s*, 2H, NH₂), 7.78 (*dd*, *J* = 7.8, 1.4 Hz, 1H, aromatic ring), 7.26 (*t*, *J* = 7.8 Hz, 1H, aromatic ring), 6.91 (*t*, *J* = 7.8 Hz, 1H, aromatic ring), and 6.65 (*dd*, *J* = 7.8, 1.4 Hz, 1H, aromatic ring).

(2E)-1-(2-aminophenyl)-3-(4-ethoxyphenyl)-2-propen-1-one (**2**). Yellow powder (87% yield), mp 155–156°C, UV-Vis (CHCl₃) λ_{max} (nm): 257.98, 334.06, FT-IR (KBr) ν (cm⁻¹): 3387 (N–H stretching), 2268 (C–H aromatic stretching), 1628 (C=O stretching), 1514 (C=C aromatic stretching), 1145 (C–O stretching) ¹H NMR 300 Hz, (CDCl₃) δ (ppm): 7.81 (*d*, *J* = 7.8 Hz, 2H, aromatic ring), 7.23 (*d*, *J* = 7.8 Hz, 2H, aromatic ring), 8.06 (*d*, *J* = 15.2 Hz, 1H, *trans*-H), 7.27 (*d*, *J* = 15.2 Hz, 1H, *trans*-H), 6.13 (*s*, 2H, NH₂), 8.26 (*dd*, *J* = 7.8, 1.4 Hz, 1H, aromatic ring), 7.66 (*t*, *J* = 7.8 Hz, 1H, aromatic ring), 6.84 (*t*, *J* = 7.8 Hz, 1H, aromatic ring), 6.63 (*dd*, *J* = 7.8, 1.4 Hz, 1H, aromatic ring), 3.87 (*q*, *J* = 6.8 Hz, 2H, CH₂ in ethoxy), and 1.24 (*t*, *J* = 6.8 Hz, 3H, CH₃ in ethoxy).

(2E)-1-(2-aminophenyl)-3-(2,4,5-trimethoxyphenyl)-2-propen-1-one (**3**). Yellow powder (85% yield), mp 172–173°C, UV-Vis (CHCl₃) λ_{max} (nm): 294.28, 387.62, FT-IR (KBr) ν (cm⁻¹): 3326 (N–H stretching), 2298 (C–H aromatic stretching), 1586 (C=O stretching), 1545 (C=C aromatic stretching), 1224 (C–O stretching) ¹H NMR 300 Hz, (CDCl₃) δ (ppm): 7.58 (*s*, 1H, aromatic ring), 6.87 (*s*, 1H, aromatic ring), 8.01 (*d*, *J* = 15.2 Hz, 1H, *trans*-H), 7.69 (*d*, *J* = 15.2 Hz, 1H, *trans*-H), 6.05 (*s*, 2H, NH₂), 7.90 (*dd*, *J* = 7.8, 1.4 Hz, 1H, aromatic ring), 7.45 (*t*, *J* = 7.8 Hz, 1H, aromatic ring), 7.11 (*t*, *J* = 7.8 Hz, 1H, aromatic ring), 6.76 (*dd*, *J* = 7.8, 1.4 Hz, 1H, aromatic ring), and 3.79–3.83 (*s*, 9H, OCH₃).

(2E)-1-(2-aminophenyl)-3-(3,4,5-trimethoxyphenyl)-2-propen-1-one (**4**). Yellow powder (79% yield), mp 165–166°C, UV-Vis (CHCl₃) λ_{max} (nm): 284.36, 372.15, FT-IR (KBr) ν (cm⁻¹): 3512 (N–H stretching), 2436 (C–H aromatic stretching), 1601 (C=O stretching), 1556 (C=C aromatic stretching), 1123 (C–O stretching) ¹H NMR 300 Hz, (CDCl₃)

Table 1. UV-Vis and IR spectral data of **1–5**

Compound	UV-Vis λ_{max} (nm)		IR (ν , cm^{-1})				
			N–H stretching	C–H aromatic stretching	C=C aromatic stretching	C=O stretching	C–O stretching
1	234.46	318.57	3428	2536	1576	1607	—
2	257.98	334.06	3387	2268	1514	1628	1145
3	294.28	387.62	3326	2258	1545	1586	1224
4	284.36	372.15	3512	2436	1556	1601	1123
5	267.84	324.13	3389	2257	1502	1587	—

δ (ppm): 7.18 (*s*, 2H, aromatic ring), 7.78 (*d*, $J = 15.2$ Hz, 1H, *trans*-H), 7.61 (*d*, $J = 15.2$ Hz, 1H, *trans*-H), 6.11 (*s*, 2H, NH_2), 7.81 (*dd*, $J = 7.8$, 1.4 Hz, 1H, aromatic ring), 7.24 (*t*, $J = 7.8$ Hz, 1H, aromatic ring), 7.02 (*t*, $J = 7.8$ Hz, 1H, aromatic ring), 6.58 (*dd*, $J = 7.8$, 1.4 Hz, 1H, aromatic ring), and 3.82–3.68 (*s*, 9H, OCH_3).

(2E)-1-(2-aminophenyl)-3-(2-thienyl)-2-propen-1-one (**5**). Yellow powder (86% yield), mp 134–135°C, UV-Vis (CHCl_3) λ_{max} (nm): 267.84, 324.13, FT-IR (KBr) ν (cm^{-1}): 3389 (N–H stretching), 2257 (C–H aromatic stretching), 1587 (C=O stretching), 1502 (C=C aromatic stretching), ^1H NMR 300 Hz, (CDCl_3) δ (ppm): 7.23 (*d*, $J = 8.7$ Hz, 1H, thiophene ring), 7.12 (*d*, $J = 8.7$ Hz, 1H, thiophene ring), 6.90 (*t*, $J = 8.7$ Hz, 1H, thiophene ring), 7.20 (*d*, $J = 15.3$ Hz, 1H, *trans*-H), 7.65 (*d*, $J = 15.3$ Hz, 1H, *trans*-H), 6.38 (*s*, 2H, NH_2), 7.91 (*dd*, $J = 7.8$, 1.4 Hz, 1H, aromatic ring), 7.32 (*td*, $J = 7.8$, 1.4 Hz, 1H, aromatic ring), 6.88 (*brt*, $J = 7.8$ Hz, 1H, aromatic ring), and 6.51 (*dd*, $J = 7.8$, 1.4 Hz, 1H, aromatic ring).

X-ray Crystallography

Yellow needle-shaped single crystals of **2** suitable for X-ray diffraction study were obtained by recrystallization from ethanol solution by slow evaporation at room temperature after several days. A suitable single crystal was selected optically for the diffraction study. A single crystal of dimensions 0.36 mm \times 0.15 mm \times 0.09 mm was used. Crystallographic data were collected at 100.0(1) K with the Oxford Cryosystem Cobra low-temperature attachment. The data were collected using a Bruker Apex2 CCD diffractometer with a graphite monochromated $\text{Mo K}\alpha$ ($\lambda = 0.71073$ Å) radiation at a detector distance of 5 cm using APEX2 [13]. The collected data were reduced using SAINT program [13], and the empirical absorption corrections were performed using SADABS program [13]. The structures were solved by direct methods and refined by least-squares using the SHELXTL software package [14]. All non-hydrogen atoms were refined anisotropically. Amino H atoms were located in difference maps and refined isotropically whereas the remaining H atoms were placed in calculated positions with C–H = 0.93 Å for aromatic and CH, 0.97 Å for CH_2 , and 0.96 Å for CH_3 . The $U_{\text{iso}}(\text{H})$ values were constrained to be $1.5U_{\text{eq}}$ of the carrier atom for methyl H and $1.2U_{\text{eq}}$ for the remaining H atoms. A rotating group model was used for the methyl groups. The final refinement converged well. Materials for publication were prepared using SHELXTL [14], PLATON [15], and Mercury [16].

Table 2. ¹H NMR data of 1–5

Compound	¹ H NMR (δ (ppm), <i>J</i> (Hz))		
	Ring A	Trans	Ring B
1	5.62 (s, 2H, NH ₂) 7.78 (<i>dd</i> , <i>J</i> = 7.8, 1.4 Hz, 1H) 7.26 (<i>t</i> , <i>J</i> = 7.8 Hz, 1H) 6.91 (<i>t</i> , <i>J</i> = 7.8 Hz, 1H) 6.65 (<i>dd</i> , <i>J</i> = 7.8, 1.4 Hz, 1H)	8.16 (<i>d</i> , <i>J</i> = 15.2 Hz, 1H) 7.56 (<i>d</i> , <i>J</i> = 15.2 Hz, 1H)	7.64 (<i>d</i> , <i>J</i> = 7.8 Hz, 2H) 7.32 (<i>t</i> , <i>J</i> = 7.8 Hz, 2H) 7.06 (<i>t</i> , <i>J</i> = 7.8 Hz, 1H)
2	6.13 (s, 2H, NH ₂) 8.26 (<i>dd</i> , <i>J</i> = 7.8, 1.4 Hz, 1H) 7.66 (<i>t</i> , <i>J</i> = 7.8 Hz, 1H) 6.84 (<i>t</i> , <i>J</i> = 7.8 Hz, 1H) 6.63 (<i>dd</i> , <i>J</i> = 7.8, 1.4 Hz, 1H)	8.06 (<i>d</i> , <i>J</i> = 15.2 Hz, 1H) 7.27 (<i>d</i> , <i>J</i> = 15.2 Hz, 1H)	7.81 (<i>d</i> , <i>J</i> = 7.8 Hz, 2H) 7.23 (<i>d</i> , <i>J</i> = 7.8 Hz, 2H) 3.87 (<i>q</i> , <i>J</i> = 6.8 Hz, 2H, OCH ₂ CH ₃) 1.24 (<i>t</i> , <i>J</i> = 6.8 Hz, 3H, OCH ₂ CH ₃)
3	6.05 (s, 2H, NH ₂) 7.90 (<i>dd</i> , <i>J</i> = 7.8, 1.2 Hz, 1H) 7.45 (<i>t</i> , <i>J</i> = 7.8 Hz, 1H) 7.11 (<i>t</i> , <i>J</i> = 7.8 Hz, 1H) 6.76 (<i>dd</i> , <i>J</i> = 7.8, 1.4 Hz, 1H)	8.01 (<i>d</i> , <i>J</i> = 15.2 Hz, 1H) 7.69 (<i>d</i> , <i>J</i> = 15.2 Hz, 1H)	7.58 (<i>d</i> , <i>J</i> = 7.8 Hz, 1H) 6.87 (<i>d</i> , <i>J</i> = 7.8 Hz, 1H) 3.79-3.83 (s, 9H, OCH ₃)
4	6.11 (s, 2H, NH ₂) 7.81 (<i>dd</i> , <i>J</i> = 7.8, 1.6 Hz, 1H) 7.24 (<i>t</i> , <i>J</i> = 7.8 Hz, 1H) 7.02 (<i>t</i> , <i>J</i> = 7.8 Hz, 1H) 6.58 (<i>dd</i> , <i>J</i> = 7.8, 1.4 Hz, 1H)	7.78 (<i>d</i> , <i>J</i> = 15.2 Hz, 1H) 7.61 (<i>d</i> , <i>J</i> = 15.2 Hz, 1H)	7.18 (<i>d</i> , <i>J</i> = 7.8 Hz, 2H) 3.82-3.68 (s, 9H, OCH ₃)
5	6.38 (s, 2H, NH ₂) 7.91 (<i>dd</i> , <i>J</i> = 7.8, 1.4 Hz, 1H) 7.32 (<i>td</i> , <i>J</i> = 7.8, 1.4 Hz, 1H) 6.88 (<i>brrt</i> , <i>J</i> = 7.8 Hz, 1H) 6.51 (<i>dd</i> , <i>J</i> = 7.8, 1.4 Hz, 1H)	7.20 (<i>d</i> , <i>J</i> = 15.3 Hz, 1H) 7.65 (<i>d</i> , <i>J</i> = 15.3 Hz, 1H)	7.23 (<i>d</i> , <i>J</i> = 8.7 Hz, 1H) 7.12 (<i>d</i> , <i>J</i> = 8.7 Hz, 1H) 6.90 (<i>t</i> , <i>J</i> = 8.7 Hz, 1H) 8.7 Hz, 1H)

Table 3. Physical properties of 1–5

Compound	R	Formular structure	Molecular weight (g/mol)	Color	% Yield	Melting point (°C)
1	H	C ₁₅ H ₁₃ NO	223.27	Orange	92	128–129
2	OCH ₂ CH ₃	C ₁₇ H ₁₇ NO ₂	267.32	Yellow	87	155–156
3	2,4,5-OCH ₃	C ₁₈ H ₁₉ NO ₄	313.35	Yellow	85	172–173
4	3,4,5-OCH ₃	C ₁₈ H ₁₉ NO ₄	313.35	Yellow	79	165–166
5	2-thiophene	C ₁₃ H ₁₁ NOS	229.30	Yellow	86	134–135

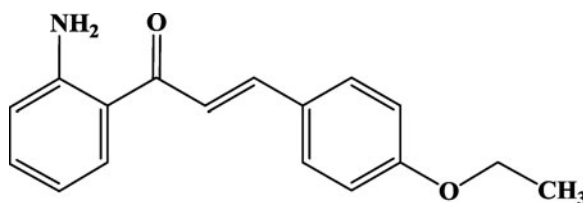
Antioxidant Activity

The DPPH scavenging method [12] was used to evaluate the antioxidant properties of the compounds. 10 μ L of the tested compounds, which was dissolved in methanol, was mixed with 190 μ L of 0.1 mM DPPH in methanol. The mixture were vigorously shaken and left to stand for 30 min in the dark. Absorbance was measured at 492 nm using Anthos 2010 Microplate Absorbance Reader. One milliliter of 0.1 mM DPPH diluted in 1 mL of methanol was used as control and 0.5 mM ascorbic acid was used as a standard reference. Neutralization of DPPH radical was calculated using the equation:

$$\% \text{Scavenging} = [(\text{Absorbance of blank} - \text{Absorbance of test}) / \text{Absorbance of blank}] \times 100$$

Antibacterial Assay

The synthesized compounds were tested against the microorganisms, *B. subtilis* (obtained from Department of Industrial Biotechnology, PSU), *S. aureus* (TISTR517) (obtained from Microbial Resources Center (MIRCEN), Bangkok, Thailand), *P. aeruginosa*, *S. faecalis*, and *S. typhi*. The last three microorganisms were obtained from Department of Pharmacognosy and Botany, PSU. The antimicrobial assay employed was the colorimetric microdilution broth technique using RPMI1640 medium and Alamar Blue as an indicator [17]. Microbial inocula were prepared as suspension in RPMI1640 medium and mixed with 1% 100 \times Alamar Blue indicator. The cell suspension was then transferred into a 96-well microliter plate (100 μ L/well except for first row which contained 190 μ L/well). The tested compound (10 μ L) dissolved in dimethyl sulfoxide at a concentration of 25 mg mL⁻¹ was added to each well of the first row and mixed well with a micropipette. Half of the mixtures of cell suspension and compounds in the first rows were then transferred to

**Figure 2.** Schematic diagram of compound 2.

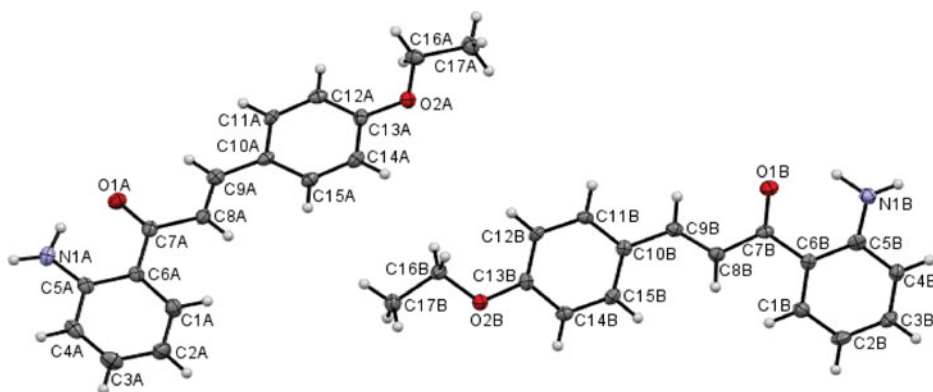


Figure 3. The molecular structure of **2**, drawn with 50% probability displacement ellipsoids and the atom numbering scheme.

the next well in the second row to perform a half-fold dilution. The dilution process was repeated as a sequence until the compounds were diluted 128 times in the last row. The excess 100 μL of the mixture in the last row was discarded. The plates were incubated at 37°C for 8–12 hr. The antibacterial activity was determined as the MIC value which was the

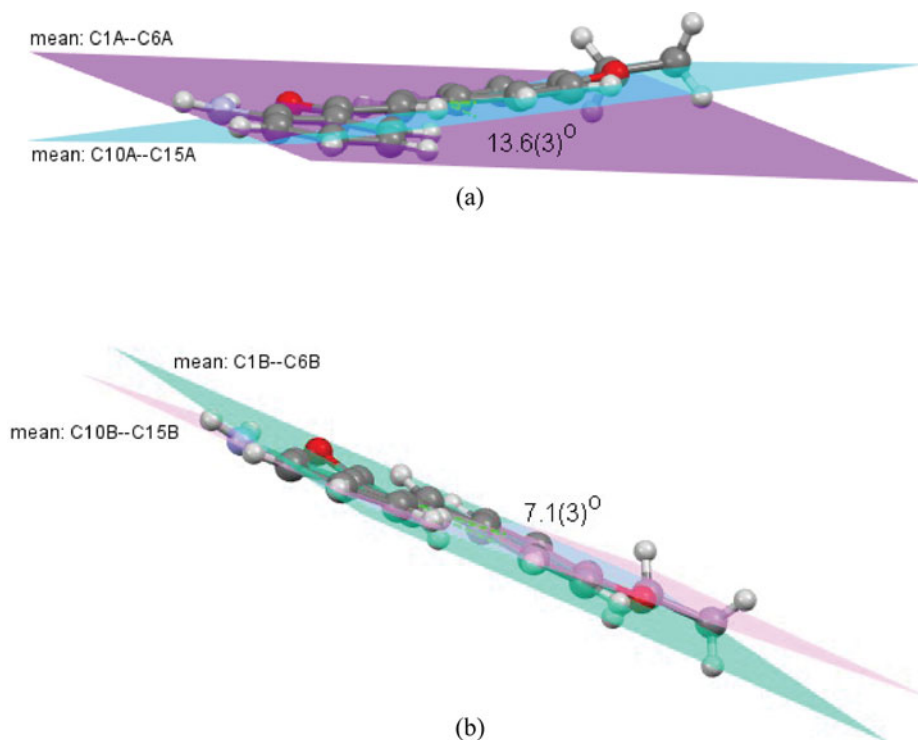


Figure 4. The dihedral angles between the mean planes through C1–C6 and C10–C15 phenyl rings in (a) molecule *A* and (b) molecule *B*.

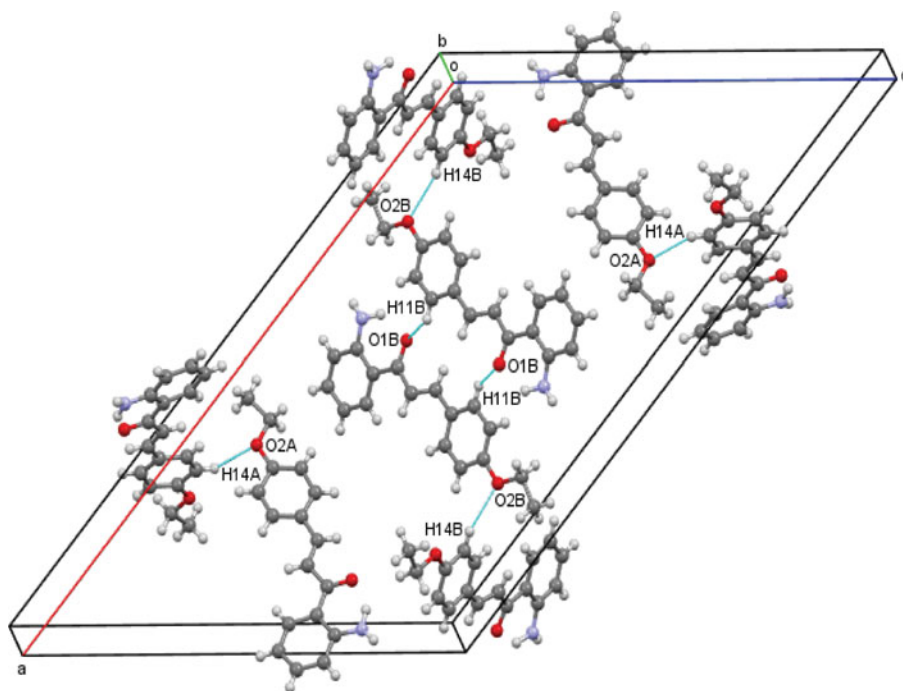


Figure 5. View of the unit cell packing of **2** approximately down the *b* axis. Hydrogen bonds are drawn as dash lines.

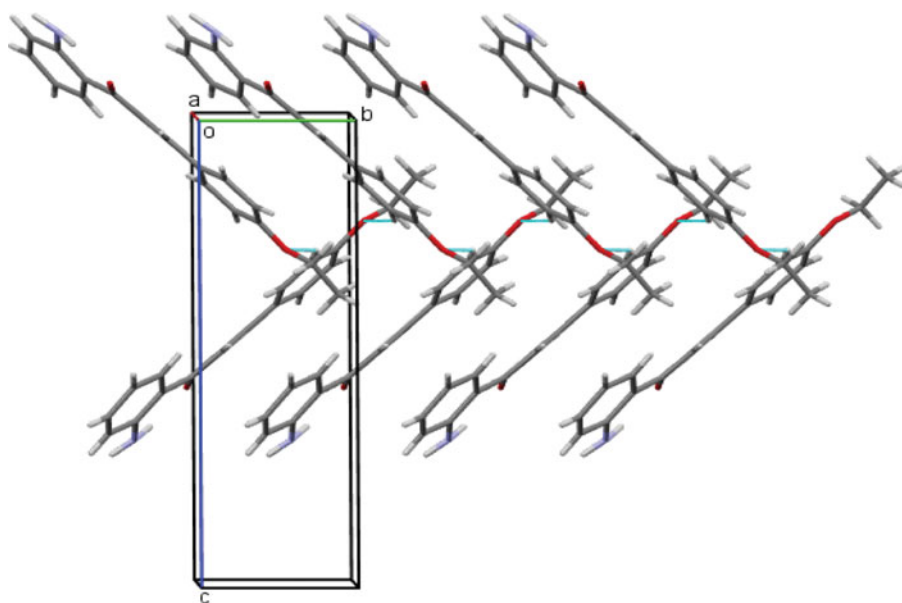


Figure 6. The crystal packing of **2**, showing a chain running along the *b* axis.

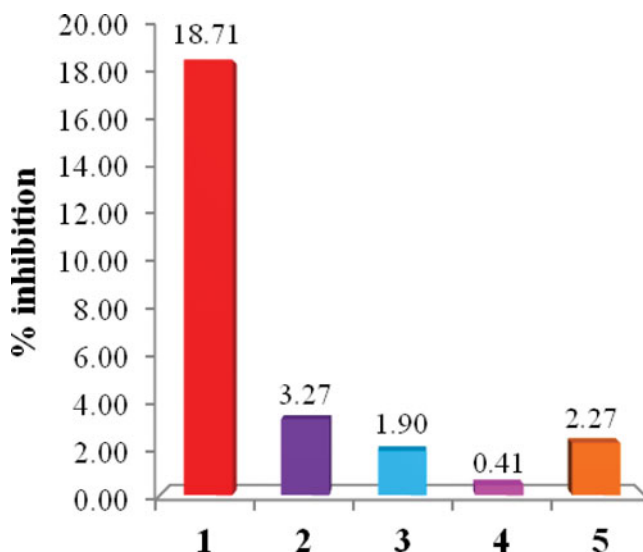


Figure 7. Percentage inhibition of free radical scavenging activity of **1–5** observed with DPPH assay using ascorbic acid as reference (92.06% inhibition).

least concentration of the compound that could inhibit the change of Alamar Blue indicator from blue to red.

Results and Discussion

UV-Vis, FT-IR, and ^1H NMR Spectra

The UV-Vis and IR spectra of compounds **1–5** were listed in Table 1 and the ^1H NMR data were listed in Table 2.

Compounds **1–5** show two UV-Vis absorbance bands (see Table 1) at the UV region of 234–294 nm which were considered to be the allowed $\pi \rightarrow \pi^*$ transitions of the aromatic system and the forbidden $n \rightarrow \pi^*$ transitions of carbonyl, and another band in the region of 318–388 nm was the allowed $\pi \rightarrow \pi^*$ transition with intramolecular charge transfer (ICT) to the enone system [18,19].

The IR data of compounds **1–5** (Table 1) show that compounds **1–5** show N–H stretching around 3326–3512 cm^{-1} . The peaks of C–H and C=C aromatic stretching were observed at 2257–2536 and 1502–1576 cm^{-1} , respectively. The strong peak at 1586–1628 cm^{-1} was assigned to C=O stretching. Moreover, C–O stretching of **2–4** was observed at 1123–1224 cm^{-1} .

The ^1H NMR data of **1–5** were presented in Table 2. All the synthesized compounds which are related structures showed a similar NMR spectra pattern. Two *doublet* signals of *trans* protons at δ 7.20–8.16 ppm with coupling constant $J = 15.2$ – 15.3 Hz of the enone system confirming the successful condensation between acetophenone and benzaldehyde were observed. The signals of aromatic protons of 2-aminophenyl ring were observed at δ 6.05–8.26 ppm and protons of amino group appeared as a singlet around δ 5.62–6.38 ppm. For compound **1**, protons of phenyl ring showed three signals at δ 7.06–7.64 ppm. For compound **2**, the signals of aromatic protons appeared at 7.23–7.81 ppm whereas the

Table 4. Crystal data and structure refinement for **2**

CCDC reference no.	CCDC 996589
Empirical formula	C ₁₇ H ₁₇ NO ₂
Formula weight	267.32
Crystal system, space group	Monoclinic, <i>P</i> 2 ₁ / <i>n</i>
Temperature (K)	100.0(1)
<i>a</i> , <i>b</i> , <i>c</i> (Å)	32.804(7), 4.9972(11), 21.7173(3)
β (°)	128.440(4)
<i>V</i> (Å ³)	2788.4(10)
<i>Z</i>	8
Calculated density (Mg m ⁻³)	1.274
Radiation type, wavelength (Å)	Mo <i>K</i> α, 0.71073
Absorption coefficient (mm ⁻¹)	0.083
Crystal form, color	needle, yellow
Crystal size (mm)	0.36 × 0.15 × 0.09
Diffractometer	CCD area detector diffractometer
Final <i>R</i> indices [<i>I</i> > 2σ(<i>I</i>)]	<i>R</i> ₁ = 0.1194, <i>wR</i> ₂ = 0.3476
<i>R</i> indices (all data)	<i>R</i> ₁ = 0.1448, <i>wR</i> ₂ = 0.3619
Reflections collected/unique	6074 / 6074 [<i>R</i> (int) = 0.0060]
θ range for data collection (°)	2.39–26.99
Limiting indices	–41 < = <i>h</i> < = 32, –6 < = <i>k</i> < = 6, –26 < = <i>l</i> < = 27
Refinement method	Full-matrix least-squares on <i>F</i> ²
Data/restraints/parameters	6074/0/380
Completeness to θ = 26.99	99.4%
<i>F</i> (000)	1136
Goodness-of-fit on <i>F</i> ²	1.111
Largest difference in peak and hole (e Å ⁻³)	0.715 and –0.676

signals of ethoxy protons appeared at 3.81 (*q*) and 1.24 (*t*) ppm. In compounds **3** and **4**, two singlet aromatic proton signals were observed at 6.87 and 7.58 ppm for **3** and the singlet of two equivalent protons of **4** were present at 7.18 ppm and the methoxy protons of **3** and **4** were observed at 3.68–3.83 ppm. For compound **5**, the thiophene protons showed three signals at 6.90–7.23 ppm. In addition, the physical properties of compounds **1**–**5** were also given in Table 3.

Single Crystal X-ray Analysis

X-ray diffraction of **2** (see Fig. 2) was performed revealing its molecular structure which was shown in Fig. 3. The crystal data of **2** are summarized in Table 4. The bond distances and angles of **2** are of normal values [20] and were listed in Table 5. There are two crystallographic independent molecules *A* and *B* in the asymmetric unit of **2** (Fig. 3) with the same conformation but slightly difference in bond angles. The molecular structure of **2** exists in *trans* configuration with respect to the C8=C9 double bond [1.355(8) Å in molecule *A* and 1.333(8) Å in molecule *B*] which can be indicated by the torsion angle

Table 5. Bond lengths (Å), angles (°), and torsion angles (°) for **2**

Bond lengths Molecule <i>A</i>		Molecule <i>B</i>	
O1A-C7A	1.233(7)	O1B-C7B	1.237(7)
O2A-C13A	1.354(7)	O2B-C13B	1.369(7)
O2A-C16A	1.434(7)	O2B-C16B	1.432(7)
N1A-C5A	1.358(7)	N1B-C5B	1.377(7)
C6A-C7A	1.475(8)	C6B-C7B	1.487(7)
C7A-C8A	1.474(8)	C7B-C8B	1.467(8)
C8A-C9A	1.355(8)	C8B-C9B	1.333(8)
C9A-C10A	1.456(8)	C9B-C10B	1.462(8)
C16A-C17A	1.517(8)	C16B-C17B	1.504(8)
N1A-H1NA	0.96(9)	N1B-H1NB	0.91(6)
N1A-H2NA	0.94(11)	N1B-H2NB	1.03(9)
Bond angles			
C13A-O2A-C16A	117.7(4)	C13B-O2B-C16B	117.7(4)
C5A-C6A-C7A	120.8(5)	C5B-C6B-C7B	121.0(5)
O1A-C7A-C8A	119.4(5)	O1B-C7B-C8B	120.4(5)
O1A-C7A-C6A	121.1(5)	O1B-C7B-C6B	120.5(5)
C8A-C7A-C6A	119.5(5)	C8B-C7B-C6B	119.2(5)
C9A-C8A-C7A	119.8(5)	C9B-C8B-C7B	121.9(5)
C8A-C9A-C10A	127.7(5)	C8B-C9B-C10B	126.8(5)
O2A-C16A-C17A	107.2(5)	O2B-C16B-C17B	107.2(5)
Torsion angles			
N1A-C5A-C6A-C7A	2.0(8)	N1B-C5B-C6B-C7B	2.8(8)
C5A-C6A-C7A-O1A	−4.3(8)	C1B-C6B-C7B-O1B	−166.7(5)
C1A-C6A-C7A-O1A	175.2(5)	C5B-C6B-C7B-O1B	10.5(8)
C1A-C6A-C7A-C8A	−5.1(8)	C1B-C6B-C7B-C8B	12.0(8)
O1A-C7A-C8A-C9A	−6.2(8)	O1B-C7B-C8B-C9B	10.1(8)
C6A-C7A-C8A-C9A	174.1(5)	C6B-C7B-C8B-C9B	−168.7(5)
C7A-C8A-C9A-C10A	178.0(5)	C7B-C8B-C9B-C10B	178.5(5)
C8A-C9A-C10A-C11A	179.0(6)	C8B-C9B-C10B-C11B	168.0(6)
C8A-C9A-C10A-C15A	−1.9(9)	C8B-C9B-C10B-C15B	−13.0(9)
C13A-O2A-C16A-C17A	178.5(5)	C13B-O2B-C16B-C17B	179.4(5)

C7—C8—C9—C10 = 178.0(5)° in molecule *A* and 178.5(5)° in molecule *B*. The molecule is twisted with the interplanar angle between the two phenyl rings being 13.6(3)° and 7.1(3)° in molecules *A* and *B*, respectively (see Fig. 4). The propenone unit (C7-C9/O1) is almost planar with the torsion angle O1—C7—C8—C9 = −6.2(8)° in molecule *A* and 10.1(8)° in molecule *B*. The mean plane through the propenone bridge makes the dihedral angles of 6.1(4)° and 8.0(4)° with the C1—C6 and C10—C15 phenyl rings, respectively in molecule *A* whereas the corresponding values are 8.2(4)° and 14.2(4)° in molecule *B*. The ethoxy group of each molecule is also coplanar with the attached benzene ring with the torsion angle C13—O2—C16—C17 = −178.5(5)° in molecule *A* and 179.4(8)° in molecule *B*. In both molecules *A* and *B*, each of intramolecular N1—H2N...O1 hydrogen bond (Table 6)

Table 6. Hydrogen bond lengths (Å) and angles (°) for **2**

D—H...A	<i>d</i> (D—H)	<i>d</i> (H...A)	<i>d</i> (D...A)	∠ D—H...A
N1A—H1NA...N1B ⁱ	0.96(9)	2.19(9)	3.135(7)	171(5)
N1B—H1NB...N1A ⁱⁱ	0.91(6)	2.36(6)	3.251(7)	167(7)
N1A—H2NA...O1A	0.95(13)	1.79(11)	2.610(8)	144(13)
N1B—H2NB...O1B	1.03(11)	1.85(9)	2.651(7)	132(9)
C14A—H14A...O2A ⁱⁱⁱ	0.93	2.53	3.258(9)	135
C14B—H14B...O2B ^{iv}	0.93	2.59	3.382(9)	143
C16A—H16B...Cg ₂ ^v	0.97	2.79	3.577(7)	139
C16B—H16D...Cg ₄ ^{vi}	0.97	2.70	3.502(6)	140

Symmetry codes: ⁱ1/2+*x*, 3/2−*y*, 3/2+*z*, ⁱⁱ−1/2+*x*, 1/2−*y*, −3/2+*z*, ⁱⁱⁱ1/2−*x*, 1/2+*y*, 3/2−*z*, ^{iv}1/2−*x*, −1/2+*y*, 1/2−*z*, ^v*x*, −1+*y*, *z*, and ^{vi}*x*, 1+*y*, *z*. Cg₂ and Cg₄ are the centroids of C10A—C15A and C10B—C15B rings, respectively.

generates S(6) ring motif [21]. This intramolecular N—H...O hydrogen bond helps to stabilize the planarity of the structure. The crystal is solidated by N—H...N hydrogen bonds together with C—H...O and C—H... π weak interactions involving 4-ethoxyphenyl rings (Table 6).

The crystal packing of **2** was depicted in Fig. 5, the two adjacent molecules of **2** are linked by C—H...O interactions (Table 6), forming V-shape chains running along the *b*-axis (Fig. 6).

Antioxidant Activity

The DPPH antioxidant assay was performed using the DPPH scavenging method and compared to ascorbic acid as a standard reference. The results were presented in Fig. 7.

Table 7. Antimicrobial activity of compounds **1–5**

Compounds	Antibacterial activity MIC (μ g/mL)							
	Gram-positive bacteria ^a					Gram-negative bacteria ^b		
	<i>B. subtilis</i>	<i>S. aureus</i>	<i>E. faecalis</i>	MRSA	VRE	<i>S. typhi</i>	<i>S. sonei</i>	<i>P. aeruginosa</i>
1	>300	>300	>300	>300	>300	>300	>300	>300
2	>300	>300	>300	>300	>300	>300	>300	>300
3	>300	>300	>300	>300	>300	>300	>300	>300
4	300	>300	>300	300	>300	>300	>300	>300
5	>300	>300	>300	>300	>300	>300	>300	>300
Vancomycin	<2.34	<2.34	<2.34	<2.34	<2.34	<2.34	<2.34	<2.34

^aBacillus subtilis, Staphylococcus aureus, Enterococcus faecalis TISTR 459, methicillin-resistant Staphylococcus aureus (MRSA) ATCC 43300, vancomycin-resistant Enterococcus faecalis (VRE) ATCC 51299.

^bSalmonella typhi, Shigella sonei and Pseudomonas aeruginosa.

Compounds **1–5** showed weakly antioxidant activity with the percentage inhibition of free radical scavenging activity in the range of 0.41%–18.71%. Compound **1** which has no substituent group on the B ring (Fig. 1) showed the highest antioxidant activity with 18.71% inhibition. In general, chalcones were reported to possess biological and antioxidant activities which was associated with the α,β -unsaturated carbonyl group. However, our results showed that compounds **2–5** do not possess interesting antioxidant activity which may indicate that the substituent groups in compounds **2–5** may not be suitable for inducing the compound to exhibit antioxidant activity. Moreover, the intramolecular N—H...O hydrogen bond between amino and enone groups (Fig. 3) may result in the prohibition of the α,β -unsaturated carbonyl moiety to be reactive.

Antibacterial Activity

Compounds **1–5** were screened for *in vitro* antibacterial activity against gram-positive and gram-negative bacteria as compared with the vancomycin standard. Preliminary results as shown in Table 7 indicate that none of compounds **1–5** exhibited promising antibacterial activities against the tested bacterial strains.

Funding

P.R. and S.C. thank the Thailand Research Fund through the Royal Golden Jubilee Ph.D. Program (grant no. PHD/0314/2552) and the Center of Excellence for Innovation in Chemistry (PERCH-CIC), Office of the Higher Education, Ministry of Education for financial support. The authors extend their appreciation to Universiti Sains Malaysia for the APEX DE2012 grant no. 1002/PFIZIK/910323 and the Deanship of Scientific Research at the King Saud University for funding the work through the research group project no. RGP-VPP-207.

Supplementary Material

CIF file containing complete information on the studied structure was deposited with the Cambridge Crystallographic Data Center, CCDC No. 996589, and is freely available upon request from the following web site: www.ccdc.cam.ac.uk/data_request/cif or by contacting the Cambridge Crystallographic Data Centre, 12, Union Road, Cambridge CB2 1EZ, UK; fax: +44 1223 336033; email: deposit@ccdc.cam.ac.uk.

References

- [1] Alan, L., & Miller, N. D. (1996). *Altern. Med. Rev.*, *1*, 103–111.
- [2] Ozyurek, M., Bekasoglu, B., Guclu, K., & Apak, R. (2009). *Anal. Chim. Acta.*, *636*, 42–50.
- [3] Nishida, J., & Kawabata, J. (2006). *Biosci. Biotechnol. Biochem.*, *70*, 193–202.
- [4] Nielsen, S. F., Boesen, T., Larsen, M., Schønning, K., & Kromann, H. (2004). *Bioorg. Med. Chem.*, *12*, 3047–3054.
- [5] Batovska, D. et al. (2007). *Eur. J. Med. Chem.*, *42*, 87–92.
- [6] Won, S. J. et al. (2005). *Eur. J. Med. Chem.*, *40*, 103–112.
- [7] Tewtrakul, S., Subhadhirasakul, S., Puripattanavong, J., & Panphadung, T. (2003). *Songklanakarin J. Sci. Technol.*, *25*, 503–508.
- [8] Romagnoli, R. et al. (2008). *Bioorg. Med. Chem.*, *16*, 5367–5376.
- [9] Jung, Y. J., Son, K. I., Oh, Y. E., & Noh, D.-Y. (2008). *Polyhedron*, *27*, 861–867.
- [10] Niu, C. G., Guan, A. L., Zeng, G. M., Liu, Y.-G., & Li, Z.-W. (2006). *Anal. Chim. Acta.*, *577*, 264–270.

- [11] Anto, R. J. et al. (1995). *Cancer. Lett.*, 97, 33–37.
- [12] Molyneux, P. (2004). *Songklanakarin J. Sci. Technol.*, 26, 211–219.
- [13] Bruker, *APEX2, SAINT and SADABS* (2009). Bruker AXS Inc., Madison, Wisconsin, USA.
- [14] Sheldrick, G. M. (2008). *Acta Cryst.*, A64, 112.
- [15] Spek, A. L. (2009). *Acta Cryst.*, D65, 148.
- [16] Macrae, C. F. et al. (2006). *Appl Cryst.*, 39, 453–457.
- [17] Kanjana-Opas, A. (2002). New antifungal compounds from marine Fungi. Ph.D. Thesis, University of California, San Diego, USA.
- [18] Zhang, J., Xu, Z., Wei, Y., Shuang, S., & Dong, C. (2008). *Spectrochim. Acta. A.*, 70, 888–891.
- [19] Gaber, M., El-Daly, S. A., Fayed, T. A., & El-Sayed, Y. S. (2008). *Opt. Laser. Technol.*, 40, 528–537.
- [20] Allen, F. H. et al. (1987). *J. Chem. Soc. Perkin Trans. 2*, S1–19.
- [21] Bernstein, J., Davis, R.E., Shimoni, L., & Chang, N.-L. (1995). *Angew. Chem. Int. Ed. Engl.*, 34, 1555–1573.